Pair-distribution function and its coupling-constant average for the spin-polarized electron gas

John P. Perdew
Department of Physics and Quantum Theory Group, Tulane University, New Orleans, Louisiana 70118

Yue Wang
Department of Chemistry, University of North Carolina, Chapel Hill, North Carolina 27599

(Received 24 July 1992)

The pair-distribution function g describes physical correlations between electrons, while its average $\bar{g}$ over coupling constant generates the exchange-correlation energy. The former is found from the latter by $g=(1-a_0\partial/\partial a_0)\bar{g}$, where a_0 is the Bohr radius. We present an analytic representation of $\bar{g}$ (and hence g) in real space for a uniform electron gas with density parameter r_s and spin polarization ζ. This expression has the following attractive features: (1) The exchange-only contribution is treated exactly, apart from oscillations we prefer to ignore. (2) The correlation contribution is correct in the high-density ($r_s\to 0$) and nonoscillatory long-range ($R\to\infty$) limits. (3) The value and cusp are properly described in the short-range ($R\to 0$) limit. (4) The normalization and energy integrals are respected. The result is found to agree with the pair-distribution function g from Ceperley's quantum Monte Carlo calculation. Estimates are also given for the separate contributions from parallel and antiparallel spin correlations, and for the long-range oscillations at a high finite density.

I. INTRODUCTION AND OUTLINE

The pair-distribution function g of an electronic system is an observable, while its average $\bar{g}$ over coupling constant e^2 (where e is the charge of an electron) generates the exchange-correlation energy.[1-3] The electron gas with uniform spin densities $(n_\uparrow, n_\downarrow)$ provides an important limit in which these distribution functions may be studied. In this work, we will construct an accurate analytic representation for the uniform gas $\bar{g}$, and test it by comparing the corresponding g with that found in a Monte Carlo calculation.[4] We need an accurate analytic representation of the uniform gas $\bar{g}$ as an input to the nonempirical construction[5,6] of a generalized gradient approximation for the exchange-correlation energy of a nonuniform system. Our $\bar{g}$ should also be useful for the construction of other nonlocal spin-density functionals, e.g., the weighted density approximation.[7,8]

For any electronic system, the pair-distribution function (which depends upon e^2 only through the Bohr radius $a_0=\hbar^2/me^2$) is[1-3]

$$g(a_0,\mathbf{r},\mathbf{r}')=1+\langle\Psi_{e^2}|\delta\hat{n}(\mathbf{r})\delta\hat{n}(\mathbf{r}')-n(\mathbf{r})\delta(\mathbf{r}'-\mathbf{r})|\Psi_{e^2}\rangle/n(\mathbf{r})n(\mathbf{r}')\ , \tag{1}$$

where Ψ_{e^2} is the ground-state wave function with spin densities $n_\uparrow(\mathbf{r})$, $n_\downarrow(\mathbf{r})$ $(n=n_\uparrow+n_\downarrow)$, and $\delta\hat{n}(\mathbf{r})=\hat{n}(\mathbf{r})-n(\mathbf{r})$ is the density fluctuation operator. Physically, $n(\mathbf{r}')g(a_0,\mathbf{r},\mathbf{r}')d^3r'$ is the expected number of electrons in volume element d^3r' at $\mathbf{r}'$, given that there is an electron at position $\mathbf{r}$. Thus g is non-negative.

The average of g over coupling constant is

$$\bar{g}(a_0,\mathbf{r},\mathbf{r}')=\frac{1}{e^2}\int_0^{e^2}d\lambda\, g(\hbar^2/m\lambda,\mathbf{r},\mathbf{r}')\ , \tag{2}$$

where the ground-state spin densities are held fixed by a fictitious local external potential while the coupling constant λ is turned off. At $\lambda=0$, the wave function Ψ_λ becomes a noninteracting Kohn-Sham wave function and $g(\hbar^2/m\lambda,\mathbf{r},\mathbf{r}')=g_x+g_c$ reduces to the exchange-only pair-distribution function g_x. The exchange-correlation energy of Kohn-Sham density functional theory is[1-3]

$$E_{xc}=E_x+E_c=\frac{e^2}{2}\int d^3r\int d^3r'\frac{n(\mathbf{r})n(\mathbf{r}')}{|\mathbf{r}'-\mathbf{r}|}[\bar{g}(a_0,\mathbf{r},\mathbf{r}')-1]\ . \tag{3}$$

To recast Eq. (2) in a useful differential form, multiply both sides by e^2, differentiate with respect to e^2, and change variable from e^2 to a_0. The result is

$$g(a_0,\mathbf{r},\mathbf{r}')=(1-a_0\partial/\partial a_0)\bar{g}(a_0,\mathbf{r},\mathbf{r}')\ . \tag{4}$$

The uniform electron gas is characterized by the dimensionless parameters r_s and ζ, where

$$n=k_F^3/3\pi^2=3/4\pi(r_sa_0)^3\ , \tag{5}$$

$$\zeta=(n_\uparrow-n_\downarrow)/n\ . \tag{6}$$

Its exchange-only pair-distribution function $g_x(\zeta,k_F|\mathbf{r}'-\mathbf{r}|)$ is independent of a_0, while its correlation contribution $g_c(r_s,\zeta,k_F|\mathbf{r}'-\mathbf{r}|)$ depends upon a_0 via r_s. Equation (4) becomes

$$g(r_s,\zeta,k_FR)=(1+r_s\partial/\partial r_s)\bar{g}(r_s,\zeta,k_FR)\ . \tag{7}$$

Here $R\equiv|\mathbf{r}'-\mathbf{r}|$, and k_F is the Fermi wave vector of Eq. (5). Fourier transformation (wave-vector analysis) of Eq. (7) yields Eq. (90) of Ref. 9.

The exchange-only pair-distribution function

$g_x(\zeta,k_FR)$ is presented in Sec. II. Its exact closed form displays long-range ($R\to\infty$) oscillations which are absent from small systems such as atoms and molecules. In Sec. II, we report a nonoscillatory model $\langle g_x\rangle$ which displays all the other principal features of g_x.

Wang and Perdew[9] used the random-phase approximation (RPA), which is exact in the high-density or small-wave-vector limits, to uncover a simple scaling relationship for the wave-vector analysis of the correlation contribution $\bar{g}_c$ in these limits. Fourier transformation back to real space gives the high-density or nonoscillatory long-range limit of $\bar{g}_c$ as a function of a single argument (scaled distance). In Sec. III, we report an analytic representation of this function.

Section IV discusses the short-range ($R\to 0$) part of $\bar{g}_c$. We present a simple analytic expression for $\bar{g}_c(r_s,\zeta,0)$, based upon Yasuhara's summation of ladder diagrams.[10] Then the familiar cusp condition[11] on g is used to construct a modified cusp condition on $\bar{g}$. These results are of special relevance to nonuniform systems, where the value and cusp of g and $\bar{g}$ in the limit of $\mathbf{r}'\to\mathbf{r}$ are expected[6,12] to be those of a uniform electron gas whose spin densities $n_\uparrow$ and $n_\downarrow$ are the ones found at position $\mathbf{r}$ in the nonuniform system.

Section V unifies the long- and short-range behaviors into a single analytic representation for $\langle\bar{g}_c\rangle$. From this, we obtain $\langle g_c\rangle$ via Eq. (7). We show that our g agrees at short and intermediate range ($R/r_sa_0\lesssim 2$) with the result of Ceperley's quantum Monte Carlo calculation[4] for $r_s=2,5,10$ and $\zeta=0$ and 1. Moreover, our expressions are usefully transparent, revealing the underlying physics of the pair-distribution function.

Section VI estimates the contributions from parallel and antiparallel spin correlation. Finally, Appendix A suggests a possible way to restore the long-range oscillations of g_c for the case of finite but high density n.

Although other analytic representations of g or $\bar{g}$ are available in the literature, none suits our purpose. Contini, Mazzone, and Sacchetti[13] presented a model for g (not $\bar{g}$) with good nonoscillatory long-range behavior. Chacón and Tarazona[8] reported an expression for $\bar{g}$ which is not exact for either g_x or $\bar{g}_c$ in the high-density limit (where g_x dominates). Neither of those representations extends to the spin-polarized case $\zeta\neq 0$. Wang and Perdew[9] constructed a Padé approximation for the wave-vector analysis of $\bar{g}$, but that expression cannot be Fourier transformed analytically back to real space; moreover, a numerical Fourier transform shows that the value and cusp of $\bar{g}$ at $R=0$ are not accurately reproduced. Thus it is necessary to construct a new analytic representation which preserves the principal features of the exact $\bar{g}$.

II. EXCHANGE-ONLY PAIR-DISTRIBUTION FUNCTION

The exact exchange-only pair distribution function for the uniform gas is

$$g_x(\zeta,k_FR)=1+\tfrac{1}{2}\{(1+\zeta)^2J[(1+\zeta)^{1/3}k_FR]+(1-\zeta)^2J[(1-\zeta)^{1/3}k_FR]\}\ , \tag{8}$$

where

$$J(y)=-\frac{9}{2}\left[\frac{\sin y-y\cos y}{y^3}\right]^2 . \tag{9}$$

It has the following important properties: (1) Since $J\le 0$, the "exchange hole density" $n(g_x-1)$ is nonpositive. (2) Since

$$\frac{4}{3\pi}\int_0^\infty dy\,y^2J(y)=-1\ , \tag{10}$$

the exchange hole density integrates to -1:

$$\int_0^\infty dR\,4\pi R^2n(g_x-1)=-1\ . \tag{11}$$

(3) Since

$$\tfrac{8}{9}\int_0^\infty dy\,y\,J(y)=-1\ , \tag{12}$$

the exchange energy per electron is

$$\frac{e^2}{2}\int_0^\infty dR\,4\pi R^2\frac{1}{R}n[g_x-1]=-\frac{3e^2k_F}{4\pi}\ . \tag{13}$$

(4) Since for small y

$$J(y)\to-\tfrac{1}{2}+\tfrac{1}{10}y^2+\cdots\ , \tag{14}$$

the short-range behavior is

$$g_x(\zeta,k_FR)\to\tfrac{1}{2}(1-\zeta^2)+\frac{(1+\zeta)^{8/3}+(1-\zeta)^{8/3}}{20}\times(k_FR)^2+\cdots\ . \tag{15}$$

(5) Since for large y

$$J(y)\to-\frac{9}{2}\frac{\cos^2y}{y^4}+\cdots=-\frac{9}{4y^4}-\frac{9\cos(2y)}{4y^4}+\cdots\ , \tag{16}$$

the nonoscillatory part of the long-range behavior is

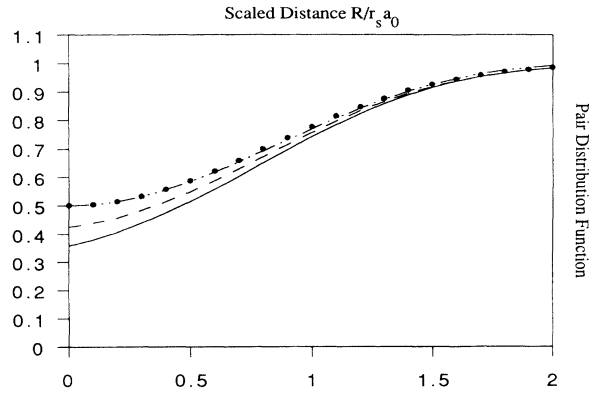

FIG. 1. Nonoscillatory part of the pair-distribution function $\langle g\rangle$ (solid curve) and its coupling constant average $\langle\bar{g}\rangle$ (dashed curve), for a uniform electron gas with density parameter $r_s=0.5$ and spin polarization $\zeta=0$. The high-density limit of $\langle g\rangle$ or $\langle\bar{g}\rangle$ is the exchange-only pair-distribution function $\langle g_x\rangle\approx g_x$ (dots).

$$g_x(\zeta,k_FR)\to 1-\frac{9\phi}{4(k_FR)^4}+\cdots\ , \tag{17}$$

where

$$\phi(\zeta)\equiv\frac{(1+\zeta)^{2/3}+(1-\zeta)^{2/3}}{2}\ . \tag{18}$$

A nonoscillatory model $\langle g_x\rangle$ with the other properties listed above is obtained by replacing $J(y)$ with

$$\langle J(y)\rangle=-\frac{A}{y^2}\frac{1}{1+\frac{4}{9}Ay^2}+\left[\frac{A}{y^2}+B+Cy^2\right]e^{-Dy^2}\ , \tag{19}$$

where $A=0.59$, $B=-0.543\,54$, $C=0.027\,678$, and $D=0.188\,43$. For small and intermediate R ($R/r_sa_0\lesssim 2$), $\langle g_x\rangle$ and g_x are identical for most practical purposes (Fig. 1). The first term of Eq. (19) is long ranged, while the second is purely short ranged. Equation (19) is a microcosm of the kind of analytical expression we shall develop for $\langle\bar{g}_c\rangle$ in Secs. III–V.

III. CORRELATION HOLE AT LONG RANGE OR HIGH DENSITY

Wang and Perdew[9] found that the high-density ($n\to\infty$) limit of the correlation hole scales as

$$n\bar{g}_c(r_s,\zeta,k_FR)\to\frac{\phi^3(\phi k_s)^2}{a_0}\frac{\bar{f}_1(v)}{4\pi v^2}\ , \tag{20}$$

where $\phi(\zeta)$ is given by Eq. (18),

$$k_s=(4k_F/\pi a_0)^{1/2}=\kappa r_s^{1/2}k_F \tag{21}$$

is the Thomas-Fermi screening wave vector [with $\kappa=(4/3\pi)(9\pi/4)^{1/3}$], and $v=\phi k_sR$. The same expression gives the long-range ($R\to\infty$) nonoscillatory limit. The function $\bar{f}_1(v)$ has been evaluated numerically [see Eqs. (7), (34), (37), and (42) of Ref. 9], and fitted[5] to the Padé form

$$\bar{f}_1(v)=\frac{a_1+a_2v+a_3v^2}{1+b_1v+b_2v^2+b_3v^3+b_4v^4}\ , \tag{22}$$

where $a_1=-0.1244$, $a_2=0.027\,032$, $a_3=0.002\,341\,7$, $b_1=0.2199$, $b_2=0.086\,664$, $b_3=0.012\,858$, $b_4=0.0020$. Equation (22) provides a fit that is accurate $v>1$, but less so for $0<v<1$; as a result, the integral $\int_0^\infty dv\,\bar{f}_1(v)$, which should vanish, turns out to be 0.009 514.

Now

$$\langle\bar{g}_c(r_s,\zeta,k_FR)\rangle\to\kappa^{-1}\phi^3r_s\bar{f}_1(\kappa\phi r_s^{1/2}k_FR)/(k_FR)^2\ . \tag{23}$$

With the help of Eq. (7), we find

$$\langle g_c(r_s,\zeta,k_FR)\rangle\to\kappa^{-1}\phi^3r_sf_1(\kappa\phi r_s^{1/2}k_FR)/(k_FR)^2\ , \tag{24}$$

where

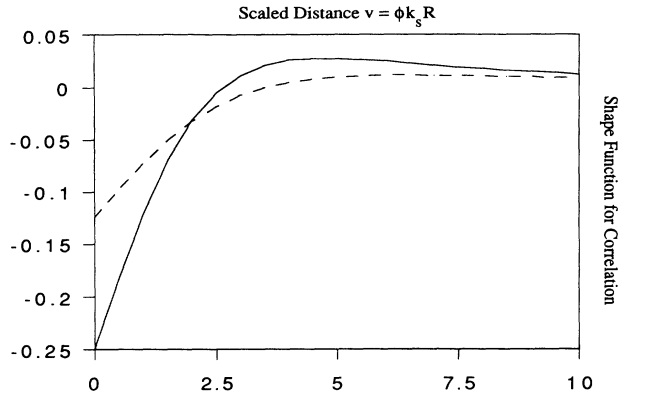

FIG. 2. Shape functions $f_1(v)$ (solid curve) and $\bar{f}_1(v)$ (dashed curve) for the high-density limit (23) and (24) of the correlation contribution to the pair-distribution function g and its coupling-constant average $\bar{g}$ in a uniform electron gas.

$$f_1(v)=2\bar{f}_1(v)+\frac{1}{2}v\frac{d}{dv}\bar{f}_1(v)\ . \tag{25}$$

Figure 2 compares the shape functions $\bar{f}_1(v)$ and $f_1(v)$. Note that $\bar{f}_1/f_1$ varies from $\frac{1}{2}$ in the limit $v\to 0$ to 1 in the limit $v\to\infty$.

As expected for any system,[12] the large-R nonoscillatory asymptote of g_c or $\bar{g}_c$ for the electron gas, $2.25\phi/(k_FR)^4$, just cancels that of g_x-1 from Eq. (17). This asymptote is of order r_s^0 or e^0, while the small-R asymptote of Eq. (23) or (24) is of order r_s or e^2 as expected from perturbation theory. The R^{-2} singularity of the small-R asymptote indicates the need for a special treatment of the short-range behavior. We shall present a sophisticated treatment in Secs. IV and V. For now we note that a sharp cutoff of all contributions to the correlation energy of Eq. (41) from k_FR/ϕ less than some constant, using the high-density limit of Eq. (23), produces a correlation energy which diverges as

$$\frac{e^2}{a_0}(0.0311)\phi^3\ln r_s\ ,$$

where $r_s\to 0$. This result is essentially the exact high-density limit.[9]

IV. CORRELATION HOLE AT SHORT RANGE

We begin with the value of the pair-distribution function at the origin. Yasuhara[10] made an approximate evaluation of the electron-electron ladder interactions and found

$$g(r_s,\zeta=0,k_FR=0)=\frac{1}{2}\left[\sum_{i=0}^{\infty}\frac{(\kappa^2r_s)^i}{i!(i+1)!}\right]^{-2}\ . \tag{26}$$

We have evaluated the coupling-constant average

$$\bar{g}(r_s,\zeta=0,k_FR=0)=\frac{1}{r_s}\int_0^{r_s}dr_s'g(r_s',\zeta=0,k_FR=0) \tag{27}$$

numerically, and fitted the result to a simple Padé form

$$\bar{g}(r_s,\zeta=0,k_FR=0)=\frac{1}{2}\frac{1+\alpha r_s}{1+\beta r_s+\alpha\beta r_s^2}\ , \tag{28}$$

with $\alpha=0.193$ and $\beta=0.525$. Then Eqs. (7) and (28) imply

$$g(r_s,\zeta=0,k_FR=0)=\frac{1}{2}\frac{1+2\alpha r_s}{(1+\beta r_s+\alpha\beta r_s^2)^2}\ . \tag{29}$$

Table I shows that these Padé forms are accurate enough for practical purposes.

We adopt the exchange-only spin dependence of Eq. (15) for the full pair-distribution function at the origin:

$$g(r_s,\zeta,k_FR=0)=(1-\zeta^2)g(r_s,\zeta=0,k_FR=0)\ . \tag{30}$$

Equation (30) is clearly correct in the limits $\zeta=0$ and 1. Defining the correlation contribution $g_c=g-g_x$, we find that $\bar{g}_c(r_s,\zeta,k_FR=0)/g_c(r_s,\zeta,k_FR=0)$ varies from $\frac{1}{2}$ in the high-density limit to 1 in the low-density limit, consistent with the results for $\bar{f}_1/f_1$ from Sec. III.

Arising from the Coulomb repulsion between electrons (and thus a pure correlation effect), the Kimball cusp condition is[11]

$$dg/dR\,|_{R=0}=g/a_0\,|_{R=0} \tag{31}$$

or

$$\partial g/\partial(k_FR)|_0=\frac{4}{3\pi\kappa}r_sg|_0\ . \tag{32}$$

Similarly $\bar{g}$ obeys a modified cusp condition

$$\partial\bar{g}/\partial(k_FR)|_0=\frac{4}{3\pi\kappa}r_sH\bar{g}|_0\ , \tag{33}$$

where H is a function of r_s. The differential equation for H is found by applying $(1+r_s\partial/\partial r_s)$ to both sides of (33), and using Eq. (7) to equate the result to (32):

$$\frac{\bar{g}}{g}\bigg|_0 r_s\frac{\partial H}{\partial r_s}+\left[1+\frac{\bar{g}}{g}\bigg|_0\right]H=1\ . \tag{34}$$

TABLE I. Pair-distribution functions g and $\bar{g}$ at the origin for a spin-unpolarized ($\zeta=0$) electron gas with density parameter r_s. The Padé approximants (29) and (28) are compared to "exact" values from Eqs. (26) and (27). The cusps $g'=\partial g/\partial(k_FR)|_0$ from Eqs. (32) and (33) are also evaluated for the Padé forms.

r_s	g		$\bar{g}$		g'	$\bar{g}'$
	Padé	"Exact"	Padé	"Exact"		
0.01	0.497	0.497	0.498	0.498	0.003	0.001
0.1	0.468	0.468	0.484	0.484	0.024	0.012
0.5	0.360	0.362	0.426	0.427	0.094	0.052
1	0.262	0.266	0.367	0.369	0.137	0.085
2	0.147	0.150	0.282	0.285	0.153	0.117
5	0.039	0.033	0.160	0.160	0.101	0.124
10	0.009	0.004	0.089	0.087	0.047	0.097
20	0.002	0.000	0.047	0.044	0.017	0.062
100	0.000	0.000	0.010	0.009	0.001	0.016

Instead of solving this equation exactly, we use the Padé forms (28) and (29) to find H in the high- ($r_s\to0$) and low- ($r_s\to\infty$) density limits, then interpolate between them:

$$H=\frac{1+\gamma r_s}{2+\delta r_s+\varepsilon r_s^2}\ , \tag{35}$$

where $\gamma=0.3393$, $\delta=0.9$, and $\varepsilon=0.101\,61$. The approximation (35) makes the left-hand side of Eq. (34) deviate from 1 by less than 0.1% for all r_s.

V. ANALYTIC MODEL FOR THE CORRELATION HOLE

Following the paradigm of Eq. (19), we now combine the long-range behavior of Eq. (23) with the short-range behavior from Sec. IV, to find the nonoscillatory part of the correlation contribution to the pair-distribution function averaged over coupling constant:

$$\langle\bar{g}_c(r_s,\zeta,k_FR)\rangle=\kappa^{-1}\phi^3r_s[\bar{f}_1(v)+\bar{f}_2]/(k_FR)^2\ , \tag{36}$$

where $v=\kappa\phi r_s^{1/2}k_FR$ and

$$\bar{f}_2=[-a_1-(a_2-a_1b_1)v+c_1v^2 +c_2v^3+c_3v^4+c_4v^5]e^{-d(\zeta)(k_FR/\phi)^2}\ . \tag{37}$$

The first two terms of (37) cancel the $R\to0$ singularities of $\bar{f}_1(v)/(k_FR)^2$. Note that the range of $\bar{f}_2$ is set by the range $2\pi\phi/k_F$ of the exchange hole.

The coefficient c_1 in Eq. (37) is fixed by the value of the pair-distribution function at the origin, Eqs. (28) and (30):

$$c_1=-0.001\,252\,9+0.1244p +\frac{0.613\,86(1-\zeta^2)}{\phi^5r_s^2}\left[\frac{1+\alpha r_s}{1+\beta r_s+\alpha\beta r_s^2}-1\right]\ , \tag{38}$$

where $p=d(\zeta)/(\kappa^2r_s\phi^4)$. Similarly the coefficient c_2 is fixed by the cusp condition of Eqs. (33) and (35):

TABLE II. The correlation energy per electron ε_c and its kinetic-energy part t_c for the uniform electron gas, from the expressions of Ref. 14 (hartrees).

	$\zeta=0$		$\zeta=1$	
r_s	$-\varepsilon_c$	t_c	$-\varepsilon_c$	t_c
0.01	0.1902	0.1595	0.0974	0.0820
0.1	0.1209	0.0918	0.0626	0.0480
0.5	0.0766	0.0511	0.0402	0.0272
1	0.0598	0.0367	0.0316	0.0198
2	0.0448	0.0246	0.0239	0.0136
5	0.0282	0.0124	0.0154	0.0074
10	0.0186	0.0066	0.0105	0.0042
20	0.0115	0.0032	0.0068	0.0023
100	0.0032	0.0005	0.0021	0.0004

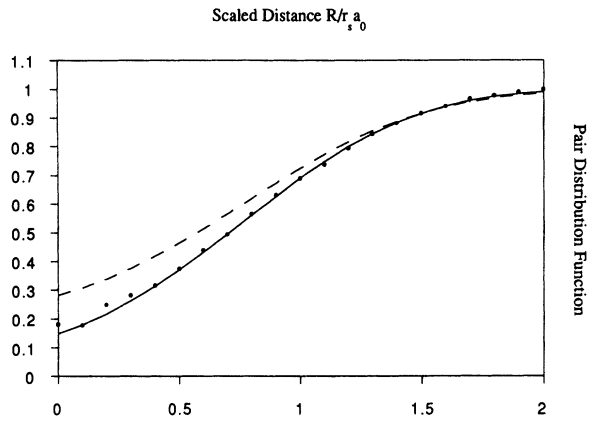

FIG. 3. Nonoscillatory part of the pair-distribution function $\langle g \rangle$ (solid curve) and its coupling-constant average $\langle \bar{g} \rangle$ (dashed curve), for a uniform electron gas with density parameter r_s and spin polarization ζ, compared with the result (heavy dots) of a quantum Monte Carlo calculation of g (Ref. 4). $r_s=2$, $\zeta=0$.

$$c_2=0.003\,389\,4-0.054\,388p+0.392\,70\frac{(1-\zeta^2)}{\phi^6 r_s^{3/2}}\left[\frac{1+\gamma r_s}{2+\delta r_s+\varepsilon r_s^2}\right]\times\left[\frac{1+\alpha r_s}{1+\beta r_s+\alpha\beta r_s^2}\right] . \quad (39)$$

Finally, the coefficients c_3 and c_4 are formed by simultaneous solution of two linear equations, corresponding to the normalization integral

$$\int_0^\infty dr\, 4\pi R^2 n\bar{g}_c=0 \quad (40)$$

and the energy integral

$$\frac{e^2}{2}\int_0^\infty dR\, 4\pi R^2\frac{1}{R}n\bar{g}_c=\frac{e^2}{a_0}\varepsilon_c(r_s,\zeta) . \quad (41)$$

The right-hand side of (41) is the correlation energy per electron. We have recently proposed an accurate and

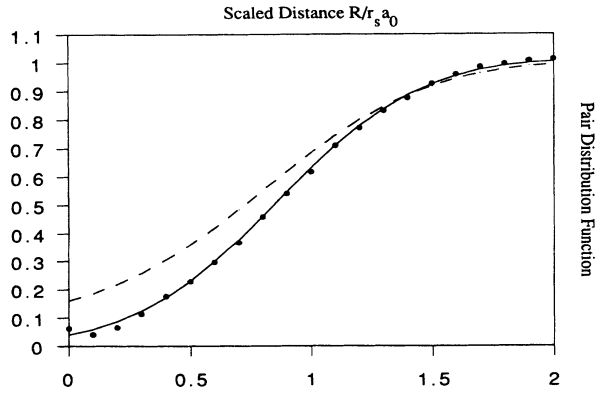

FIG. 4. Same as Fig. 3. $r_s=5$, $\zeta=0$.

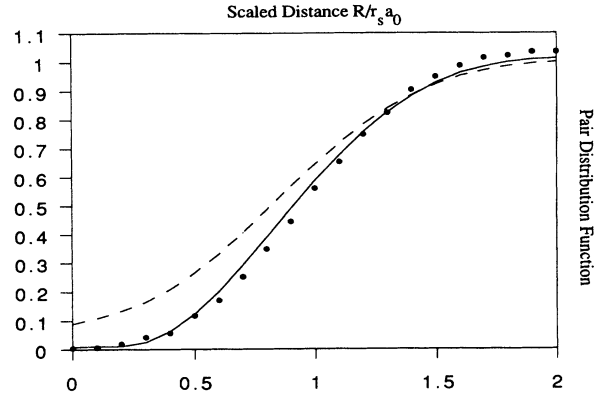

FIG. 5. Same as Fig. 3. $r_s=10$, $\zeta=0$.

simple expression[14] for the dimensionless function $\varepsilon_c(r_s,\zeta)<0$. (By rewriting Eq. (41) as an integral over $k_F R$ and invoking Eq. (7), we find

$$\frac{e^2}{2}\int_0^\infty dR\, 4\pi R^2\frac{1}{R}ng_c=\frac{e^2}{a_0}[\varepsilon_c(r_s,\zeta)-t_c(r_s,\zeta)] , \quad (42)$$

where $t_c=-\partial(r_s\varepsilon_c)/\partial r_s>0$ is the kinetic-energy contribution to $\varepsilon_c(r_s,\zeta)$. Table II presents numerical values for ε_c and t_c. Clearly t_c arises from $\bar{g}_c-g_c$. Since $\lim_{r_s\to 0} g_c/\bar{g}_c=2$, the high-density limit of t_c is $-\varepsilon_c$. Since $\lim_{R\to\infty} g_c/\bar{g}_c=1$, t_c is free from the most long-ranged correlations that contribute to ε_c. For generalizations of these relationships to nonuniform densities, see Eq. (4) and Ref. 15).

From Eqs. (40) and (41), we find

$$c_3=0.108\,47p^{5/2}+1.4604p^2+0.517\,49p^{3/2}-3.5297c_1p-1.9030c_2p^{1/2}+1.0685p^2\ln p+34.356\phi^{-3}\varepsilon_c(r_s,\zeta)p^2 , \quad (43)$$

$$c_4=-0.081\,596p^3-1.0810p^{5/2}-0.316\,77p^2+1.9030c_1p^{3/2}+0.764\,85c_2p-0.710\,19p^{5/2}\ln p-22.836\phi^{-3}\varepsilon_c(r_s,\zeta)p^{5/2} . \quad (44)$$

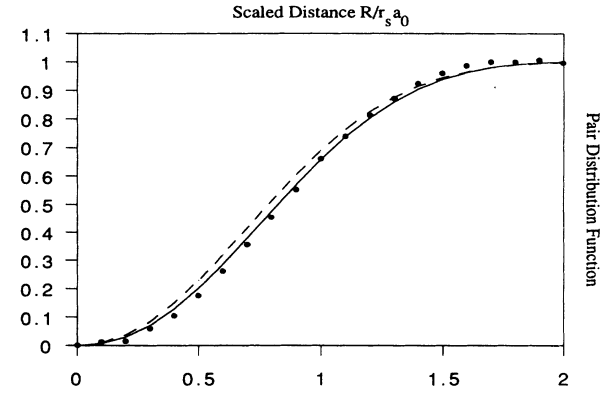

FIG. 6. Same as Fig. 3. $r_s=2$, $\zeta=1$.

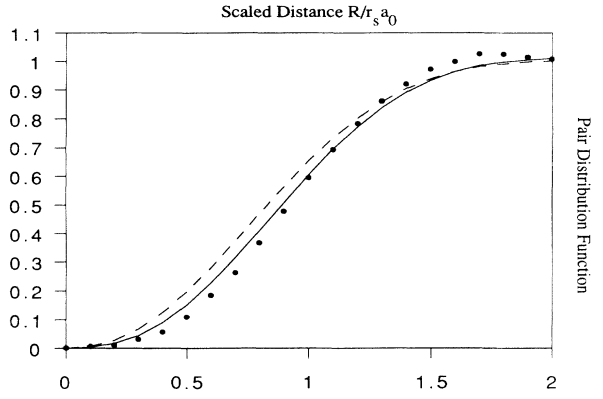

FIG. 7. Same as Fig. 3. $r_s=5$, $\zeta=1$.

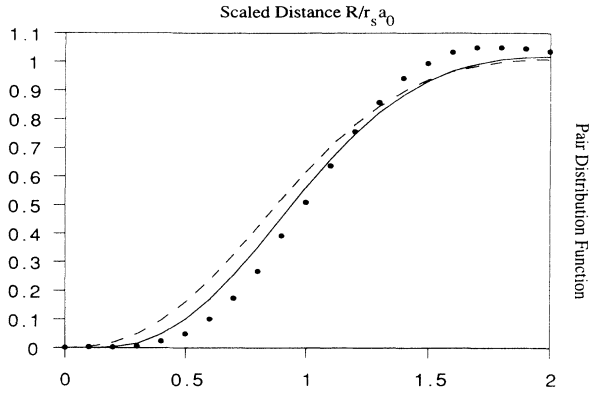

FIG. 8. Same as Fig. 3. $r_s=10$, $\zeta=1$.

The coefficient $d(\zeta)$ in Eq. (37) is left as a free parameter. We have found that

$$d(\zeta)=0.305-0.136\zeta^2 \tag{45}$$

provides a good fit of $\langle g\rangle=\langle g_x\rangle+\langle g_c\rangle$ [Eqs. (8), (19), (7), and (36)] to Ceperley's quantum Monte Carlo data[4] for g (Figs. 3–8). The fit is least satisfactory for the fully polarized ($\zeta=1$) electron gas at low density, where the Monte Carlo pair-distribution function shows the beginning of an oscillation even for small and intermediate R ($R/r_s a_0 \lesssim 2$). This energetically unimportant oscillation is not included in our model.

Our expressions reveal the underlying physics of the nonoscillatory part $\langle g\rangle$ of the pair-distribution function: The exchange-only contribution of Eqs. (8) and (19) has an amplitude of order $(r_s)^0$ and a range of one Fermi wavelength $2\pi/k_F$. In the high-density ($r_s\to 0$) limit, the correlation contribution of Eqs. (36) and (7) to $\langle\bar{g}\rangle$ or $\langle g\rangle$ has an amplitude of order r_s (whence $\langle g_c\rangle\approx 2\langle\bar{g}_c\rangle$) and a range of one screening length $1/k_s=1/(\kappa r_s^{1/2}k_F)$. In the low-density ($r_s\to\infty$) limit, the correlation contribution becomes of order $(r_s)^0$ (whence $\langle g_c\rangle\approx\langle\bar{g}_c\rangle$) with a range of $2\pi/k_F$, like the exchange contribution. The high-density behavior of $\langle g\rangle$ is shown in Fig. 2.

Because of the truncated expansion in Eq. (37), the analytic model of this section breaks down for very low densities ($r_s>10$). Appendix B presents expressions for this low-density regime.

VI. SPIN ANALYSIS OF THE PAIR-DISTRIBUTION FUNCTION

Following Ref. 11, the pair-distribution function of the uniform gas may be spin-analyzed as

$$g=\left[\frac{1+\zeta}{2}\right]^2 g^{\uparrow\uparrow}+\left[\frac{1-\zeta}{2}\right]^2 g^{\downarrow\downarrow}+\left[\frac{1-\zeta^2}{2}\right] g^{\uparrow\downarrow}\ . \tag{46}$$

A model for $g^{\sigma\sigma'}$, which permits us to use Eqs. (8), (19), and (36) while respecting the normalization integrals,[11]

$$\int_0^\infty dR\ 4\pi R^2 n_\sigma [g_{\sigma\sigma'}-1]=-\delta_{\sigma,\sigma'}\ , \tag{47}$$

is

$$g^{\uparrow\uparrow}(r_s,\zeta,k_F R)=g[r_s,1,(1+\zeta)^{1/3}k_F R/2^{1/3}]\ , \tag{48}$$

$$g^{\downarrow\downarrow}(r_s,\zeta,k_F R)=g[r_s,-1,(1-\zeta)^{1/3}k_F R/2^{1/3}]\ , \tag{49}$$

$$g^{\uparrow\downarrow}(r_s,\zeta,k_F R)=\frac{2}{1-\zeta^2}\left[g(r_s,\zeta,k_F R)-\left[\frac{1+\zeta}{2}\right]^2 g(r_s,1,(1+\zeta)^{1/3}k_F R/2^{1/3})-\left[\frac{1-\zeta}{2}\right]^2 g(r_s,-1,(1-\zeta)^{1/3}k_F R/2^{1/3})\right]\ . \tag{50}$$

Equations (48)–(50) are exact at the exchange-only level (where $g_x^{\uparrow\downarrow}=1$) for all R, and beyond this level for $R=0$. These equations also correctly show that the most short-ranged features of the correlation contribution g_c or $\bar{g}_c$ (i.e., the value and cusp at the origin) arise purely from antiparallel ($\uparrow\downarrow$) spin correlation, while the most long-ranged nonoscillatory feature of g_c or $\bar{g}_c$ (which cancels that of g_x-1) arises purely from parallel ($\uparrow\uparrow$ and $\downarrow\downarrow$) spin correlation. Note that Eqs. (30) and (50) make $g^{\uparrow\downarrow}(r_s,\zeta,0)=g^{\uparrow\downarrow}(r_s,0,0)$ for all ζ. Of particular interest is the problem of one down-spin electron in a sea of up-spin electrons; according to Eq. (50)

$$\lim_{\zeta\to 1} g^{\uparrow\downarrow} = [1+(k_F R/6)\partial/\partial(k_F R)]g(r_s,1,k_F R) - [\partial/\partial\zeta]g(r_s,\zeta,k_F R)|_{\zeta=1} , \quad (51)$$

where the last term carries the value and cusp at $R=0$.

From Eqs. (41) and (48)–(50), the parallel-spin contribution to the correlation energy $\varepsilon_c(r_s,\zeta)$ is predicted to be

$$\left[\left(\frac{1+\zeta}{2}\right)^{4/3}+\left(\frac{1-\zeta}{2}\right)^{4/3}\right]\varepsilon_c(r_s,1) . \quad (52)$$

For $\zeta=0$, this is typically less than half of the total $\varepsilon_c(r_s,0)$. Clearly the $\uparrow\downarrow$ contributions dominate[11] the correlation energy of the spin-unpolarized electron gas, and even more that of small systems which admit no long-range correlation.

ACKNOWLEDGMENTS

We thank Robert G. Parr for helpful discussions, and David Ceperley for sending us the unpublished pair-distribution functions from his calculation of Ref. 4. This work was supported in part by the National Science Foundation under Grant No. DMR 88-17866 (J.P.P.), and in part by the Petroleum Research Fund of the American Chemical Society (Y.W.).

APPENDIX A: LONG-RANGE OSCILLATION OF THE CORRELATION HOLE AT HIGH FINITE DENSITY

While the long-range ($R\to\infty$) nonoscillatory behavior of g_c or $\bar{g}_c$ is associated with the small-wave-vector limit $k\to 0$, the long-range oscillatory behavior arises from a discontinuity[9] of the second derivative of the wave-vector analysis at finite k ($=2k_F$ when $\zeta=0$). The relative strength of this oscillation vanishes in the high-density limit.

For a finite but high density, the random-phase approximation may suffice. Figure 2 and Table III of Isihara and Ten Seldam[16] show the long-range oscillation in $g_c^{\rm RPA}$ for $\zeta=0$. The result is at least qualitatively

$$g_c^{\rm RPA} \approx \langle g_c^{\rm RPA}\rangle + \frac{r_s(r_s+2E)}{(r_s+E)^2}[\langle g_x\rangle - g_x] , \quad (A1)$$

where $E=2\pi(9\pi/4)^{1/3}=12.06$. (The exchange-only pair-distribution function g_x and its nonoscillatory model $\langle g_x\rangle$ were presented in Sec. II.) From Eq. (7), we find the average over coupling constant

$$\bar{g}_c^{\rm RPA} \approx \langle \bar{g}_c^{\rm RPA}\rangle + \frac{r_s}{r_s+E}[\langle g_x\rangle - g_x] . \quad (A2)$$

Note that the oscillation of $g_c^{\rm RPA}$ or $\bar{g}_c^{\rm RPA}$ vanishes in the high-density limit ($r_s\to 0$). In the low-density limit ($r_s\to\infty$), we find within RPA (but not beyond it) a tendency for the oscillation of $\bar{g}_c$ to cancel that of g_x: $g_x+\bar{g}_c^{\rm RPA}\to\langle g_x\rangle+\langle\bar{g}_c^{\rm RPA}\rangle$. In fact, the low-density limit of the RPA correlation hole completely "screens out"[9] the exchange hole on the scale of the Fermi wavelength $2\pi/k_F$: $n(g^{\rm RPA}-1)\to-\delta(\mathbf{r}'-\mathbf{r})$.

The only oscillation found in RPA is of the Friedel type. Beyond RPA, a second oscillation of the incipient-Wigner-crystal type appears at low density. We have not attempted to represent this second oscillation here.

APPENDIX B: NONOSCILLATORY MODEL FOR LOW DENSITY

A reasonable model for the low-density limit of $\langle g\rangle$ or $\langle\bar{g}(r_s,\zeta,k_F R)\rangle$ is

$$\langle\bar{g}(\infty,\zeta,y)\rangle = 1-(1+\mu y+\tfrac{1}{2}\mu^2 y^2+\nu y^3)e^{-\mu y} , \quad (B1)$$

where $\mu=1.0891$ and $\nu=-0.1825$. Equation (B1) has a plausible shape, is properly independent of ζ, and respects the normalization and energy integrals in this limit.

For $r_s>10$, where the model of Sec. V breaks down, we propose the interpolation formula

$$\langle\bar{g}_c(r_s,\zeta,k_F R)\rangle = x\langle\bar{g}_c(10,\zeta,k_F R)\rangle + (1-x)[\langle\bar{g}(\infty,\zeta,\chi k_F R)\rangle - \langle\bar{g}_x(\zeta,\chi k_F R)\rangle] , \quad (B2)$$

where x is fixed by the value at the origin:

$$x = 5.591(1+\alpha r_s)/(1+\beta r_s+\alpha\beta r_s^2) , \quad (B3)$$

and χ by the energy integral:

$$\chi^2 = \frac{(1-x)\{0.8959-0.2291[(1+\zeta)^{4/3}+(1-\zeta)^{4/3}]\}}{[-r_s\varepsilon_c(r_s,\zeta)+10x\varepsilon_c(10,\zeta)]} . \quad (B4)$$

[1]D. C. Langreth and J. P. Perdew, Solid State Commun. **17**, 1425 (1975).
[2]O. Gunnarsson and B. I. Lundqvist, Phys. Rev. B **13**, 4274 (1976).
[3]D. C. Langreth and J. P. Perdew, Phys. Rev. B **15**, 2884 (1977).
[4]D. M. Ceperley, Phys. Rev. B **18**, 3126 (1978); D. M. Ceperley and B. J. Alder, Phys. Rev. Lett. **45**, 566 (1980).
[5]J. P. Perdew, in *Electronic Structure of Solids '91*, edited by P. Ziesche and H. Eschrig (Akademie Verlag, Berlin, 1991), p. 11.
[6]J. P. Perdew and Y. Wang (unpublished). This work extends to correlation the real-space cutoff construction applied to exchange by J. P. Perdew and Y. Wang, Phys. Rev. B **33**, 8800 (1986).
[7]O. Gunnarsson, M. Jonson, and B. I. Lundqvist, Phys. Rev. B **20**, 3136 (1979).
[8]E. Chacón and P. Tarazona, Phys. Rev. B **37**, 4013 (1988).
[9]Y. Wang and J. P. Perdew, Phys. Rev. B **44**, 13 298 (1991). The high-density limit for the correlation energy $\varepsilon_c(r_s,\zeta)$ has been evaluated exactly by Y. Wang and J. P. Perdew, Phys. Rev. B **43**, 8911 (1992); and by G. G. Hoffman, *ibid.* **45**, 8730 (1992).
[10]H. Yasuhara, Solid State Commun. **11**, 1481 (1972).

[11]A. K. Rajagopal, J. C. Kimball, and M. Banerjee, Phys. Rev. B **18**, 2339 (1978); J. C. Kimball, Phys. Rev. A **7**, 1648 (1973).
[12]D. C. Langreth and J. P. Perdew, Phys. Lett. **92A**, 451 (1982).
[13]V. Contini, G. Mazzone, and F. Sacchetti, Phys. Rev. B **33**, 712 (1986).
[14]J. P. Perdew and Y. Wang, Phys. Rev. B **45**, 13 244 (1992).
[15]A. Görling, M. Levy, and J. P. Perdew, Phys. Rev. B (to be published).
[16]A. Isihara and C. A. Ten Seldam, Physica **76**, 153 (1974).